

Journal of Materials Chemistry A

Accepted Manuscript



This is an *Accepted Manuscript*, which has been through the Royal Society of Chemistry peer review process and has been accepted for publication.

Accepted Manuscripts are published online shortly after acceptance, before technical editing, formatting and proof reading. Using this free service, authors can make their results available to the community, in citable form, before we publish the edited article. We will replace this *Accepted Manuscript* with the edited and formatted *Advance Article* as soon as it is available.

You can find more information about *Accepted Manuscripts* in the [Information for Authors](#).

Please note that technical editing may introduce minor changes to the text and/or graphics, which may alter content. The journal's standard [Terms & Conditions](#) and the [Ethical guidelines](#) still apply. In no event shall the Royal Society of Chemistry be held responsible for any errors or omissions in this *Accepted Manuscript* or any consequences arising from the use of any information it contains.



Journal Name

ARTICLE

Ag₂O Modified g-C₃N₄ for Highly Efficient Photocatalytic Hydrogen Generation under Visible Light Irradiation

Ming Wu, Jun-Min Yan*, Xue-Wei Zhang, Ming Zhao, and Qing Jiang

Received 00th January 20xx,
Accepted 00th January 20xx

DOI: 10.1039/x0xx00000x

www.rsc.org/

The Ag₂O modified g-C₃N₄ (Ag₂O/g-C₃N₄) is synthesized by a facial hydrothermal reaction. The as-prepared Ag₂O/g-C₃N₄ shows the efficient photocatalytic property on hydrogen evolution by water splitting under visible light irradiation, which is about 274 times higher than that of pure g-C₃N₄, and is even much better than that of Pt/g-C₃N₄. More importantly, Ag₂O/g-C₃N₄ also demonstrates a relatively good recycling stability for photocatalytic hydrogen evolution.

1. Introduction

Photocatalysts for chemical conversion of solar energy have been vigorously pursued since the discovery of photolysis of water into hydrogen (H₂) and oxygen (O₂),¹ which has been recognized as a potential answer to the global energy crisis and environmental pollution.² An ideal photocatalyst should possess an appropriate band edge position for overall water splitting into H₂ or O₂ and a relative narrow band-gap for efficient utilization of visible light.³ To date, numerous metal-based inorganic photocatalysts have been explored for water decomposition, such as metal-oxides,⁴⁻⁷ metal-(oxy)sulfides,⁸⁻¹¹ and metal-(oxy)nitrides.¹²⁻¹⁴ However, most of them are moderately active only in the ultraviolet region, and are still plagued by low thermal and chemical stabilities. Therefore, developing the new photocatalysts for water splitting with high activity and good stability under visible light is highly desirable but remained as a big challenge.

Recently, polymeric graphitic carbon nitride (g-C₃N₄) with a narrow band-gap of about 2.7 eV has been proposed as a promising “metal-free” photocatalyst for H₂ or O₂ production via water splitting under visible light irradiation.¹⁵ g-C₃N₄ is constructed by tri-s-triazine units,¹⁶⁻¹⁸ and the strong covalent bonds between carbon (C) and nitrogen (N) atoms can lead to the high stability of g-C₃N₄ in aqueous solutions ranging from acid to alkali.¹⁹ Furthermore, g-C₃N₄ is environment benign and inexpensive relative to the metal-based photocatalysts.^{20, 21} All the above advantages endows g-C₃N₄ as a promising candidate for photocatalysis-driven application.¹⁵ However, the pristine g-C₃N₄ always shows very low activity due to the rapid recombination rate of photo-generated charge carriers.^{22, 23} To improve its photocatalytic efficiency, several methods have been employed, for example, by doping with metal or nonmetal species, such as Ag,²⁴ Au,²⁵ Fe,²⁶ K,^{22, 27} S,²⁸ B,²⁹ P,^{30, 31} I,³² and C,³³ coupling with some other semiconductors,³⁴⁻³⁷ synthesizing

mesoporous structures or nanorods,³⁸⁻⁴⁰ and sensitizing by organic dyes.⁴¹

Although significant progress has been achieved, further increase of the activity of g-C₃N₄ to promote the kinetic property of H₂ generation from water splitting is still urgently needed. Ag₂O as a promising visible-light photocatalyst for the narrow band gap of 1.2 eV, has always been used to dope with other semiconductors.⁴²⁻⁴⁷ However, there is no research on the photocatalytic hydrogen evolution by Ag₂O/g-C₃N₄ from water splitting.

In this work, by using a facile solvothermal method, Ag₂O/g-C₃N₄ composite has been successfully synthesized. The obtained composite demonstrates significantly enhanced photocatalytic activity for H₂ production than those of the pristine g-C₃N₄ and Pt/g-C₃N₄ in the triethanolamine solution under visible-light irradiation. Moreover, the present photocatalyst also shows a good stability during the recycling application.

2. Experimental

2.1 Chemicals

Melamine (C₃H₆N₆, Aladdin Chemistry, ≥99%), Silver nitrate (AgNO₃, Beijing Chemicals Works, ≥99.8%), potassium phosphate monobasic (K₂HPO₄·3H₂O, Sinopharm Chemical Reagent Co., Ltd, ≥99.8%), chloroplatinic acid hexahydrate (H₂PtCl₆·6H₂O, Sinopharm Chemical Reagent Co., Ltd, ≥37% Pt basis), triethanolamine ((HOCH₂CH₂)₃N, Aladdin Chemistry, Reagent Co., Ltd, ≥99%) were used without any purification. Ultrapure water with the specific resistance of 18.2 MΩ·cm was obtained by reversed osmosis followed by ion-exchange and filtration.

2.2 Preparation of Ag₂O/g-C₃N₄

The g-C₃N₄ powder was prepared by heating C₃H₆N₆ at 550°C for 4 h with a ramp rate of 4 °C min⁻¹ under N₂ atmosphere,¹⁵ and the obtained sample was grinded into powder in a mortar. And then, Ag₂O/g-C₃N₄ (weight ratio of Ag₂O:g-C₃N₄ is 0.83 wt %) was prepared by a facial hydrothermal

* Key Laboratory of Automobile Materials (Jilin University), Ministry of Education, Department of Materials Science and Engineering, Jilin University, Changchun 130022, China. E-mail: junminyan@jlu.edu.cn; Fax: +86-431-85095876; Tel: +86-431-85095178

reaction method as follows: g-C₃N₄ (500 mg) and AgNO₃ (6.1 mg, 0.036 mmol) were dispersed into 40 mL of water with sonication for 1 h. After that, K₂HPO₄ aqueous solution (0.1 mL, 0.18 mol L⁻¹) was added into the above solution at room temperature with magnetic stirring for 30 min. This obtained Ag₃PO₄/g-C₃N₄ suspension was placed in a Teflon-sealed autoclave (50 mL) and maintained at 160 °C for 12 h. After natural cooling, the as-prepared specimen was washed with water by 3 times. Finally, the washed specimen was dried at 60 °C for 12 h. Samples with other different weight ratios of Ag₂O/g-C₃N₄ (0.08 wt %, 0.42 wt %, 2.10 wt %, 4.20 wt %) have been prepared by the same method mentioned above.

2.3 Photocatalytic test

Reactions were carried in a Pyrex top-irradiation reaction vessel connected to a glass closed gas system. Hydrogen production was performed by dispersing 100 mg of the as-prepared catalyst in aqueous solution containing (HOCH₂CH₂)₃N (100 mL, 10 vol. %) as a sacrificial electron donor. For Pt/g-C₃N₄ sample, 0.83 wt% of Pt was loaded on the surface of g-C₃N₄ through the *in situ* photodeposition method¹⁵ by using H₂PtCl₆ as the Pt precursor. The reaction solution was evacuated to remove air completely prior to the irradiation of the 300 W xenon-lamp (CEL-HXF 300, 320 < λ < 2500 nm) with a 420 nm cutoff filter (AULIGHT). The temperature of the reaction solution was maintained below 10 °C by a flow of cooling water during the reaction. The evolved gas was analyzed by gas chromatography (GC7900) equipped with a thermal conductive detector (TCD), using N₂ as the carrier gas.

2.4 Catalyst characterization

Powder X-ray diffraction (XRD) patterns were performed on a Rigaku D/max-2500pc X-ray diffractometer with Cu Kα irradiation (λ = 1.5406 Å) by a scan rate of 2 °/min. Transmission electron microscope (TEM) together with an energy-dispersive X-ray spectroscopy (EDS) was operated by JEOL JEM-2010 microscope (accelerating voltage = 200 kV). X-ray photoelectron spectroscopy (XPS) results were obtained by an ESCALABMk II (Vacuum Generators) spectrometer using 300 W Al Kα radiation. All binding energies were referenced to C 1s peak at 284.6 eV of the surface adventitious carbon. Fourier transform infrared spectra (FTIR) of the samples were tested on a NEXUS-670 spectrometer at the room temperature. Ultraviolet-Visible (UV-Vis) diffuse reflection spectra were recorded on a UV-3600 spectrophotometer. The photoluminescence (PL) spectra were detected on a Hitachi F-7000 fluorescence spectrophotometer.

3. Results and discussion

Fig. 1a and b show the TEM images of the pure g-C₃N₄ and Ag₂O/g-C₃N₄, respectively. It can be seen that the synthesized Ag₂O/g-C₃N₄ has the similar sheet structure as the pure g-C₃N₄. However, the sizes of Ag₂O/g-C₃N₄ nanosheets are smaller than those of the pure g-C₃N₄, which may be caused by the extra high temperature hydrothermal reaction during synthesis of

Ag₂O/g-C₃N₄. From the XRD patterns of g-C₃N₄ and Ag₂O/g-C₃N₄ (Fig. 1c), It can be seen that the two specimens show the similar main peaks at 2θ of 27.5° and 12.8°, corresponding to the interlayer^{16, 48} and in-plane structures^{19, 22} of g-C₃N₄, respectively. No Ag or its related oxide has been found for Ag₂O/g-C₃N₄, which may be resulted from the low addition of Ag₂O. However, the existence of Ag₂O has been proved by the energy-dispersive X-ray spectroscopy (EDS) and high resolution XPS spectrum of Ag₂O/g-C₃N₄ (Figs. 1d, and 2a). From the EDS result, elements of Ag, C, N, O, Cu and Si can be found in Ag₂O/g-C₃N₄ (the existences of Cu and Si are attributed to the Cu grid and EDX detector, respectively). And from the Ag 3d X-

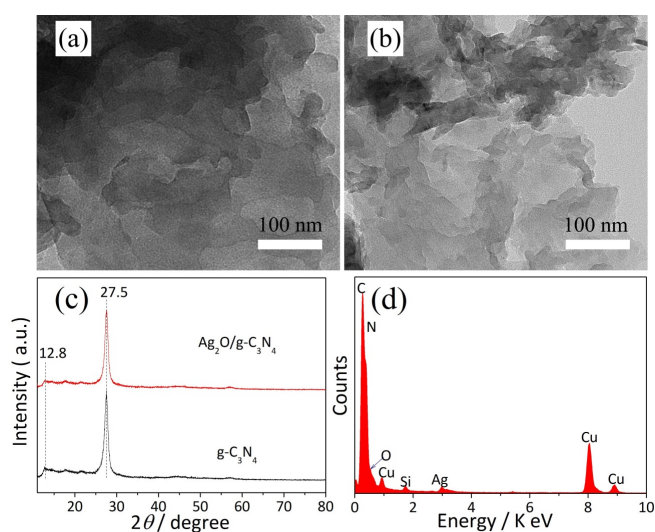


Fig. 1 TEM images of (a) pure g-C₃N₄ and (b) Ag₂O/g-C₃N₄; (c) XRD patterns of pure g-C₃N₄ and Ag₂O/g-C₃N₄; and (d) EDS pattern of Ag₂O/g-C₃N₄.

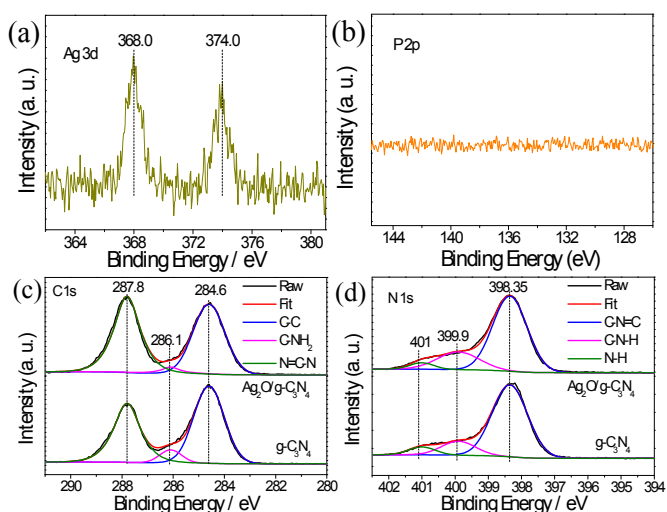


Fig. 2 High-resolution XPS spectra of (a) Ag 3d in Ag₂O/g-C₃N₄, (b) P 2p in Ag₂O/g-C₃N₄, (c) C 1s in g-C₃N₄ and Ag₂O/g-C₃N₄, and (d) N 1s in g-C₃N₄ and Ag₂O/g-C₃N₄.

-PS analysis, two peaks at 368.0 and 374.0 eV related to phase of Ag_2O can be found.⁴⁵ Additionally, no element of P has been detected by EDS and XPS analyses (Figs. 1d, and 2b). Besides, the high resolution XPS spectra of C 1s and N 1s of $\text{Ag}_2\text{O}/\text{g}-\text{C}_3\text{N}_4$ and pure $\text{g}-\text{C}_3\text{N}_4$ have been detected for comparison (Fig. 2c, d), where no obvious binding energy shift has been found between these two specimens, and all the peaks demonstrate the typical chemical states of C 1s and N 1s of $\text{g}-\text{C}_3\text{N}_4$.²² This means that the structure of $\text{g}-\text{C}_3\text{N}_4$ has not been changed or destroyed by Ag_2O addition, which is consistent with the follow FTIR analysis (Fig. 3).

As shown in Fig. 3, the chemical structure of $\text{g}-\text{C}_3\text{N}_4$ and $\text{Ag}_2\text{O}/\text{g}-\text{C}_3\text{N}_4$ are further investigated by FTIR analysis. For $\text{g}-\text{C}_3\text{N}_4$, there are three main absorption regions. The broad band peak loaded at $3000\text{--}3500\text{ cm}^{-1}$ is ascribed to the stretching vibration of N-H and O-H of physically adsorbed water.⁴⁴ The absorption peak in $1200\text{--}1700\text{ cm}^{-1}$ is attributed to the stretching vibration of CN heterocycles, while the sharp peak at 809 cm^{-1} is attributed to the typical breathing vibration of triazine unites.^{16, 19} And all the three main absorption regions of $\text{Ag}_2\text{O}/\text{g}-\text{C}_3\text{N}_4$ have no peak shift relative to pure $\text{g}-\text{C}_3\text{N}_4$, which agrees very well with the XPS result (Fig. 2c, d).

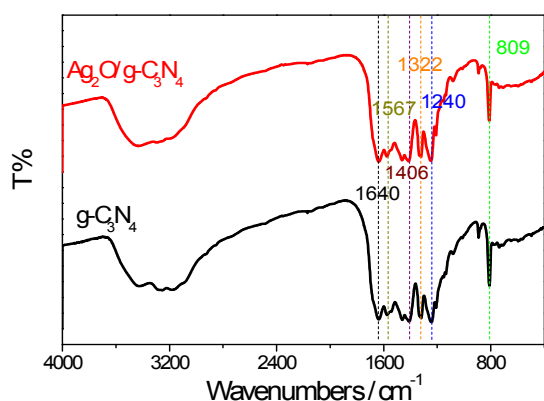


Fig. 3 FTIR spectra of pure $\text{g}-\text{C}_3\text{N}_4$ and $\text{Ag}_2\text{O}/\text{g}-\text{C}_3\text{N}_4$.

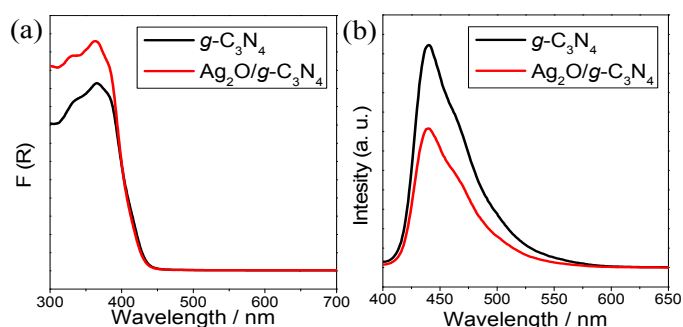


Fig. 4 (a) UV-Vis diffuse reflectance spectra of $\text{g}-\text{C}_3\text{N}_4$ and $\text{Ag}_2\text{O}/\text{g}-\text{C}_3\text{N}_4$, (b) PL spectra of $\text{g}-\text{C}_3\text{N}_4$ and $\text{Ag}_2\text{O}/\text{g}-\text{C}_3\text{N}_4$ with 370 nm excitation.

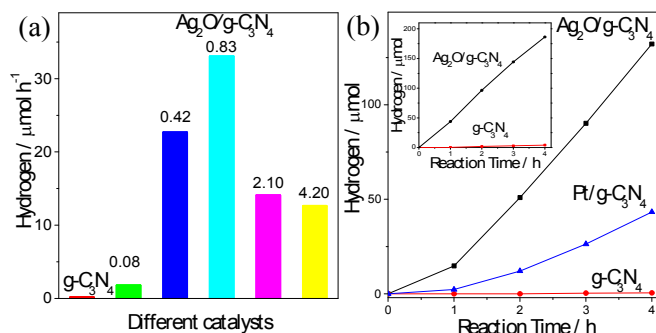


Fig. 5 (a) Hydrogen evolution rate over pure $\text{g}-\text{C}_3\text{N}_4$ and $\text{Ag}_2\text{O}/\text{g}-\text{C}_3\text{N}_4$ with different weight ratios of $\text{Ag}_2\text{O}:\text{g}-\text{C}_3\text{N}_4$ under visible light irradiation within 4 h, (b) time course of hydrogen evolution over pure $\text{g}-\text{C}_3\text{N}_4$, $\text{Ag}_2\text{O}/\text{g}-\text{C}_3\text{N}_4$ ($\text{Ag}_2\text{O}:\text{g}-\text{C}_3\text{N}_4=0.83\text{ wt}\%$) and $\text{Pt}/\text{g}-\text{C}_3\text{N}_4$ ($\text{Pt}:\text{g}-\text{C}_3\text{N}_4=0.83\text{ wt}\%$) under visible light irradiation, and (b inset) time course of hydrogen evolution over pure $\text{g}-\text{C}_3\text{N}_4$, and $\text{Ag}_2\text{O}/\text{g}-\text{C}_3\text{N}_4$ under simulated sunlight irradiation.

To investigate the electronic band structures, UV-Vis diffuse reflectance and PL spectra have been applied on the $\text{Ag}_2\text{O}/\text{g}-\text{C}_3\text{N}_4$ and pure $\text{g}-\text{C}_3\text{N}_4$ for comparison. As shown in Fig. 4a, the UV-Vis adsorption of $\text{Ag}_2\text{O}/\text{g}-\text{C}_3\text{N}_4$ has almost no red or blue shift compared with the pure $\text{g}-\text{C}_3\text{N}_4$, while its absorption intensity is higher than that of $\text{g}-\text{C}_3\text{N}_4$, indicating the higher utilization of the UV-Vis light. Fig. 4b shows the PL spectra of $\text{Ag}_2\text{O}/\text{g}-\text{C}_3\text{N}_4$ and pure $\text{g}-\text{C}_3\text{N}_4$ (as a reference) excited by 370 nm at room temperature. The pure $\text{g}-\text{C}_3\text{N}_4$ has an emission peak at around 440 nm corresponding to its band gap of about 2.82 eV. $\text{Ag}_2\text{O}/\text{g}-\text{C}_3\text{N}_4$ has much lower emission peak compared with the pure $\text{g}-\text{C}_3\text{N}_4$, which can be considered that the addition of Ag_2O can effectively hinder the recombination rate of photogenerated electron-hole pairs,⁴⁸⁻⁵⁰ and thus may benefit for photocatalytic activity of $\text{Ag}_2\text{O}/\text{g}-\text{C}_3\text{N}_4$ (*vide infra*).

Photocatalytic hydrogen evolution of the samples is evaluated under the visible light irradiation ($\lambda > 420\text{ nm}$). As shown in Fig. 5a, $\text{Ag}_2\text{O}/\text{g}-\text{C}_3\text{N}_4$ samples with different weight ratios of $\text{Ag}_2\text{O}:\text{g}-\text{C}_3\text{N}_4$ show the great higher photocatalytic activities than the pure $\text{g}-\text{C}_3\text{N}_4$, and with the best catalyst of $\text{Ag}_2\text{O}/\text{g}-\text{C}_3\text{N}_4$ ($\text{Ag}_2\text{O}:\text{g}-\text{C}_3\text{N}_4=0.83\text{ wt}\%$), hydrogen generation rate within 4 h can reach $33.04\text{ }\mu\text{mol h}^{-1}$, corresponding to 274 times higher than that of the pure $\text{g}-\text{C}_3\text{N}_4$ ($0.12\text{ }\mu\text{mol h}^{-1}$). Further increase the Ag_2O addition from 0.83 wt%, the activity of $\text{Ag}_2\text{O}/\text{g}-\text{C}_3\text{N}_4$ decreases. This decrease may be caused by the shading effect,⁵¹⁻⁵³ which can seriously hinder the absorption of incident light by $\text{g}-\text{C}_3\text{N}_4$ and decrease the surface active sites of $\text{g}-\text{C}_3\text{N}_4$. As shown in Fig. 5b, $\text{Ag}_2\text{O}/\text{g}-\text{C}_3\text{N}_4$ ($\text{Ag}_2\text{O}:\text{g}-\text{C}_3\text{N}_4=0.83\text{ wt}\%$) can generate $132.14\text{ }\mu\text{mol}$ of hydrogen within 4 h, which is much better than pure $\text{g}-\text{C}_3\text{N}_4$ ($0.49\text{ }\mu\text{mol}/4\text{ h}$) and even $\text{Pt}/\text{g}-\text{C}_3\text{N}_4$ ($43.30\text{ }\mu\text{mol}/4\text{ h}$). Furthermore, under simulated sunlight irradiation without using the cutoff filter, $\text{Ag}_2\text{O}/\text{g}-\text{C}_3\text{N}_4$ also shows excellent activity compared with $\text{g}-\text{C}_3\text{N}_4$ (Fig. 5b inset). It should be noted that pure Ag_2O has no activity for hydrogen generation from water splitting due to its more

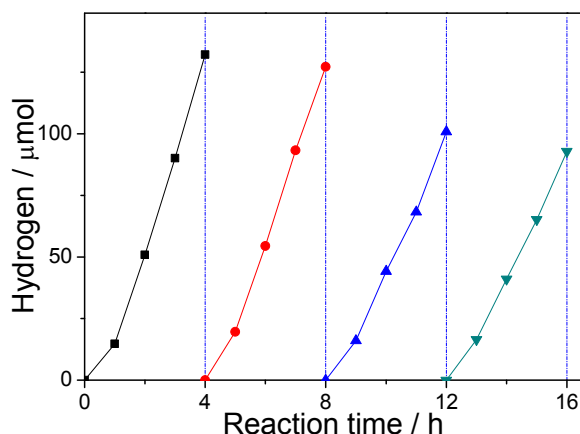


Fig. 6 Stability test of hydrogen evolution for $\text{Ag}_2\text{O}/\text{g-C}_3\text{N}_4$ under visible light irradiation ($\lambda > 420\text{nm}$).

positive level of conduction band (CB) than redox potential of H^+/H_2 .^{3, 44, 54, 55}

To test the stability of the synthesized catalysts, the recycling experiment with catalyst of $\text{Ag}_2\text{O}/\text{g-C}_3\text{N}_4$ ($\text{Ag}_2\text{O}:\text{g-C}_3\text{N}_4=0.83$ wt%) has been applied under visible light irradiation for 4 times with every period of 4 h (total reaction time is 16 h). As shown in Fig. 6, during the 4th run, 92.86 μmol hydrogen can be generated within 4 h. Although this value is slightly decreased compared with the 1st run (132.14 $\mu\text{mol}/4$ h), it is still higher than that of $\text{Pt}/\text{g-C}_3\text{N}_4$ (43.30 $\mu\text{mol}/4$ h, Fig. 5b).

To find the reason for the slight activity loss of $\text{Ag}_2\text{O}/\text{g-C}_3\text{N}_4$, FTIR is analyzed on this catalyst after its 4th recycling application. With the results shown in Fig. 7a, it is found that the structure of $\text{g-C}_3\text{N}_4$ in $\text{Ag}_2\text{O}/\text{g-C}_3\text{N}_4$ has no change or destruction after reaction. Therefore, the reduced reason might be caused by the change of Ag_2O , and this can be confirmed by the XPS result in Fig. 7b, where Ag^+ is partially reduced to be Ag^0 after the recycling experiment.^{47,56} This change in the chemical state of Ag may be resulted from the photo-reduction during the photocatalytic reaction.⁴³

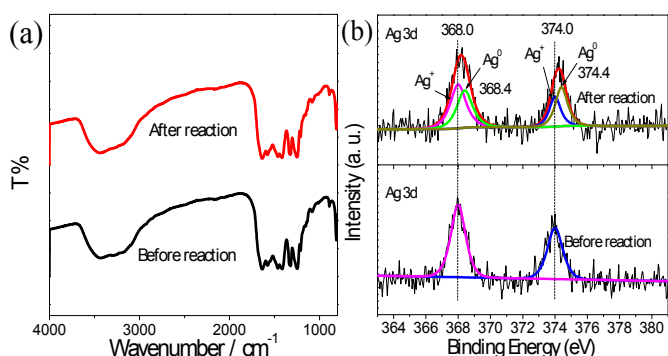


Fig. 7 (a) FTIR spectra of $\text{Ag}_2\text{O}/\text{g-C}_3\text{N}_4$ and (b) high-resolution XPS spectra of Ag 3d of $\text{Ag}_2\text{O}/\text{g-C}_3\text{N}_4$ before and after the recycling experiment.

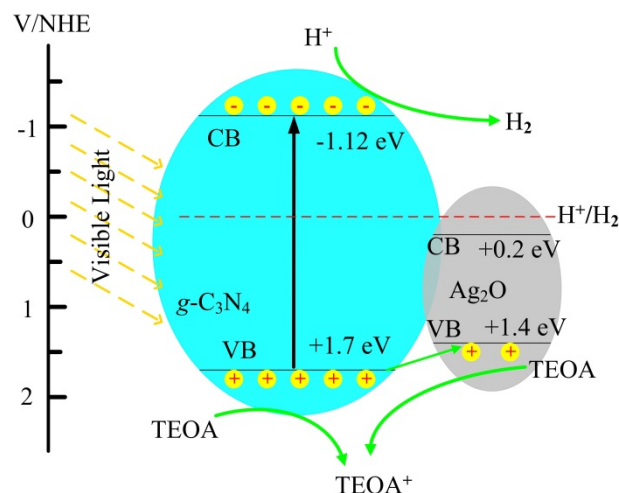


Fig. 8 Photocatalytic reaction mechanism of hydrogen evolution over $\text{Ag}_2\text{O}/\text{g-C}_3\text{N}_4$.

Based on the above analyses, the photocatalytic mechanism of $\text{Ag}_2\text{O}/\text{g-C}_3\text{N}_4$ can be explained as Fig. 8. The bottom of conduction band (CB) for $\text{g-C}_3\text{N}_4$ (-1.12 eV, vs SHE) is more negative than that of Ag_2O (0.20 eV, vs SHE), and the top of valence band (VB) for $\text{g-C}_3\text{N}_4$ (1.7 eV, vs SHE) is more positive than that of Ag_2O (1.40 eV, vs SHE).^{44,46} Under visible light irradiation, the photogenerated holes of $\text{g-C}_3\text{N}_4$ can be transferred to the higher valence band (VB) of Ag_2O .^{43, 44} However, the photogenerated electrons of $\text{g-C}_3\text{N}_4$ cannot be transferred to conduction band (CB) of Ag_2O because the redox potential of H^+/H_2 is higher than CB of Ag_2O .⁴⁴ And as the transferred holes are consumed, more photogenerated electrons could be used in photocatalytic hydrogen evolution, and thus enhance the catalytic activity.

Conclusions

In summary, we have successfully synthesized $\text{Ag}_2\text{O}/\text{g-C}_3\text{N}_4$ by a facial hydrothermal reaction. Compared with the pure $\text{g-C}_3\text{N}_4$ and even $\text{Pt}/\text{g-C}_3\text{N}_4$, the photocatalytic hydrogen evolution rate of $\text{Ag}_2\text{O}/\text{g-C}_3\text{N}_4$ under visible light irradiation has been greatly improved. Most importantly, even after 16 h of recycling experiment, $\text{Ag}_2\text{O}/\text{g-C}_3\text{N}_4$ also shows much better photocatalytic activity than that of $\text{Pt}/\text{g-C}_3\text{N}_4$. The present easy synthetic method and effective $\text{Ag}_2\text{O}/\text{g-C}_3\text{N}_4$ catalyst may provide a new idea for improving other photocatalysts in hydrogen evolution.

Acknowledgements

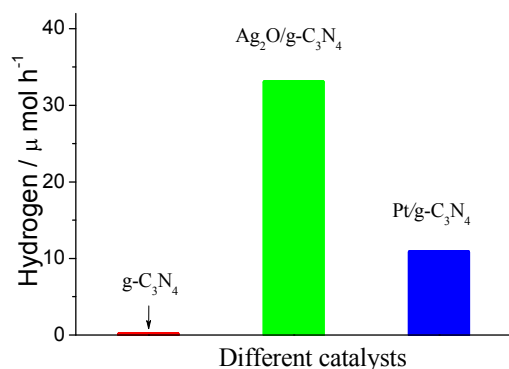
This work is supported in part by the National Natural Science Foundation of China (51471075, 51401084 and 51101070); National Key Basic Research, Development Program (2010CB631001).

Notes and references

- 1 A. Fujishima and K. Honda, *Nature*, 1972, **238**, 37-38.

- 2 R. D. Cortright, R. R. Davda and J. A. Dumesic, *Nature*, 2002, **418**, 964-967.
- 3 A. Kudo and Y. Miseki, *Chem. Soc. Rev.*, 2009, **38**, 253-278.
- 4 H. Kato and A. Kudo, *J. Phys. Chem. B*, 2002, **106**, 5029-5034.
- 5 L. Liao, Q. H. Zhang, Z. H. Su, Z. Z. Zhao, Y. N. Wang, Y. Li, X. X. Lu, D. D. Wei, G. Y. Feng, Q. K. Yu, X. J. Cai, J. M. Zhao, Z. F. Ren, H. Fang, F. Robles-Hernandez, S. Baldelli and J. M. Bao, *Nature Nanotech.*, 2014, **9**, 69-73.
- 6 X. B. Chen and S. S. Mao, *Chem. Rev.*, 2007, **107**, 2891-2959.
- 7 X. Wang, Q. Xu, M. R. Li, S. Shen, X. L. Wang, Y. H. Wang, Z. C. Feng, J. Y. Shi, H. X. Han and C. Li, *Angew. Chem. Int. Ed.*, 2012, **51**, 13089-13092.
- 8 A. Ishikawa, T. Takata, J. N. Kondo, M. Hara, H. Kobayashi and K. Domen, *J. Am. Chem. Soc.*, 2002, **124**, 13547-13553.
- 9 Y. P. Hong, J. Zhang, X. Wang, Y. J. Wang, Z. Lin, J. G. Yu and F. Huang, *Nanoscale*, 2012, **4**, 2859-2862.
- 10 X. Zong, H. J. Yan, G. P. Wu, G. J. Ma, F. Y. Wen, L. Wang and C. Li, *J. Am. Chem. Soc.*, 2008, **130**, 7176-7177.
- 11 J. Zhang, J. G. Yu, Y. M. Zhang, Q. Li and J. R. Gong, *Nano Lett.*, 2011, **11**, 4774-4779.
- 12 Z. Wang, K. Xie, L. Zhao and B. S. Zhang, *Chem. Commun.*, 2015, **51**, 2437-2439.
- 13 Y. B. Li, T. Takata, D. Cha, K. Takanabe, T. Minegishi, J. Kubota and K. Domen, *Adv. Mater.*, 2013, **25**, 125-131.
- 14 G. Hitoki, T. Takata, J. N. Kondo, M. Hara, H. Kobayashi and K. Domen, *Chem. Commun.*, 2002, 1698-1699.
- 15 X. C. Wang, K. Maeda, A. Thomas, K. Takanabe, G. Xin, J. M. Carlsson, K. Domen and M. Antonietti, *Nat. Mater.*, 2009, **8**, 76-80.
- 16 M. J. Bojdys, J. O. Müller, M. Antonietti and A. Thomas, *Chem. Eur. J.*, 2008, **14**, 8177-8182.
- 17 M. Deifallah, P. F. McMillan and F. Corà, *J. Phys. Chem. C*, 2008, **112**, 5447-5453.
- 18 M. Groenewolt and M. Antonietti, *Adv. Mater.*, 2005, **17**, 1789-1792.
- 19 S. C. Yan, Z. S. Li and Z. G. Zou, *Langmuir*, 2009, **25**, 10397-10401.
- 20 F. Dong, L. W. Wu, Y. J. Sun, M. Fu, Z. B. Wu and S. C. Lee, *J. Mater. Chem.*, 2011, **21**, 15171-15174.
- 21 S. Chu, Y. Wang, Y. Guo, J. Y. Feng, C. C. Wang, W. J. Luo, X. X. Fan and Z. G. Zou, *ACS Catal.*, 2013, **3**, 912-919.
- 22 M. Wu, J. M. Yan, X. N. Tang, M. Zhao and Q. Jiang, *ChemSusChem*, 2014, **7**, 2654-2658.
- 23 L. Ge and C. C. Han, *Appl. Catal. B*, 2012, **117-118**, 268-274.
- 24 L. Ge, C. C. Han, J. Liu and Y. F. Li, *Appl. Catal. a*, 2011, **409**, 215-222.
- 25 Y. Di, X. C. Wang, A. Thomas and M. Antonietti, *ChemCatChem*, 2010, **2**, 834-838.
- 26 X. F. Chen, J. S. Zhang, X. Z. Fu, M. Antonietti and X. C. Wang, *J. Am. Chem. Soc.*, 2009, **131**, 11658-11659.
- 27 M. Zhang, X. J. Bai, D. Liu, J. Wang and Y. F. Zhu, *Appl. Catal. B*, 2015, **164**, 77-81.
- 28 G. Liu, P. Niu, C. H. Sun, S. C. Smith, Z. G. Chen, G. Q. Lu and H. M. Cheng, *J. Am. Chem. Soc.*, 2010, **132**, 11642-11648.
- 29 Z. Z. Lin and X. C. Wang, *Angew. Chem. Inter. Ed.*, 2013, **52**, 1735-1738.
- 30 Y. P. Yuan, S. W. Cao, Y. S. Liao, L. S. Yin and C. Xue, *Appl. Catal. B*, 2013, **140-141**, 164-168.
- 31 Y. J. Zhang, T. Mori, J. H. Ye and M. Antonietti, *J. Am. Chem. Soc.*, 2010, **132**, 6294-6295.
- 32 G. G. Zhang, M. W. Zhang, X. X. Ye, X. Q. Qiu, S. Lin and X. C. Wang, *Adv. Mater.*, 2014, **26**, 805-809.
- 33 J. Liu, Y. Liu, N. Y. Liu, Y. Z. Han, X. Zhang, H. Huang, Y. Lifshitz, S. T. Lee, J. Zhong and Z. H. Kang, *Science*, 2015, **347**, 970-974.
- 34 B. Chai, T. Y. Peng, J. Mao, K. Li and L. Zan, *Physical Chemistry Chemical Physics*, 2012, **14**, 16745-16752.
- 35 L. Ge, F. Zuo, J. K. Liu, Q. Ma, C. Wang, D. Z. Sun, L. Bartels and P. Y. Feng, *J. Phys. Chem. C*, 2012, **116**, 13708-13714.
- 36 S. C. Yan, S. B. Lv, Z. S. Li and Z. G. Zou, *Dalton Trans.*, 2010, **39**, 1488-1491.
- 37 L. Y. Huang, Y. P. Li, H. Xu, Y. G. Xu, J. X. Xia, K. Wang, H. M. Li and X. N. Cheng, *RSC Adv.*, 2013, **3**, 22269-22279.
- 38 Y. W. Zhang, J. H. Liu, G. Wu and W. Chen, *Nanoscale*, 2012, **4**, 5300-5303.
- 39 J. D. Hong, X. Y. Xia, Y. S. Wang and R. Xu, *J. Mater. Chem.*, 2012, **22**, 15006-15012.
- 40 X. H. Li, J. S. Zhang, X. F. Chen, A. Fischer, A. Thomas, M. Antonietti and X. C. Wang, *Chem. Mater.*, 2011, **23**, 4344-4348.
- 41 H. J. Yan and Y. Huang, *Chem. Commun.*, 2011, **47**, 4168-4170.
- 42 H. T. Ren, S. Y. Jia, Y. Wu, S. H. Wu, T. H. Zhang and X. Han, *Ind. Eng. Chem. Res.*, 2014, **53**, 17645-17653.
- 43 M. Wu, J. M. Yan, M. Zhao and Q. Jiang, *Chempluschem*, 2012, **77**, 931-935.
- 44 M. Xu, L. Han and S. J. Dong, *ACS Appl. Mater. Interfaces*, 2013, **5**, 12533-12540.
- 45 L. Shi, L. Liang, J. Ma, F. Wang and J. Sun, *Catal. Sci. Technol.*, 2014, **4**, 758-765.
- 46 X. F. Wang, S. F. Li, H. G. Yu, J. G. Yu and S. W. Liu, *Chem. Eur. J.*, 2011, **17**, 7777-7780.
- 47 H. G. Yu, R. Liu, X. F. Wang, P. Wang and J. G. Yu, *Applied Catalysis B*, 2012, **111-112**, 326-333.
- 48 J. S. Zhang, M. W. Zhang, G. G. Zhang and X. C. Wang, *ACS Catal.*, 2012, **2**, 940-948.
- 49 J. H. Li, B. Shen, Z. H. Hong, B. Z. Lin, B. F. Gao and Y. L. Chen, *Chem. Commun.*, 2012, **48**, 12017-12019.
- 50 J. G. Hou, C. Yang, Z. Wang, W. L. Zhou, S. Q. Jiao and H. M. Zhu, *Appl. Catal. B*, 2013, **142**, 504-511.
- 51 J. G. Yu and J. R. Ran, *Energy Environ. Sci.*, 2011, **4**, 1364-1371.
- 52 Y. D. Hou, A. B. Laursen, J. S. Zhang, G. G. Zhang, Y. S. Zhu, X. C. Wang, S. Dahl, I. Chorkendorff, *Angew. Chem. Int. Ed.*, 2013, **52**, 3621-3625.
- 53 J. R. Ran, J. G. Yu and M. Jaroniec, *Green Chem.*, 2011, **13**, 2708-2713.
- 54 C. M. Liu, J. W. Liu, G. Y. Zhang, J. B. Zhang, Q. S. Wu, Y. Y. Xu and Y. Q. Sun, *RSC Adv.*, 2015, **5**, 32333-32342.
- 55 X. B. Chen, S. H. Shen, L. J. Guo and S. S. Mao, *Chem. Rev.*, 2010, **110**, 6503-6570.
- 56 J. M. Du, J. L. Zhang, Z. M. Liu, B. X. Han, T. Jiang and Y. Huang, *Langmuir*, 2006, **22**, 1307-1312.

Table of the Content



$\text{Ag}_2\text{O/g-C}_3\text{N}_4$ shows high hydrogen evolution rate from water splitting, which is much more efficient than those of $\text{g-C}_3\text{N}_4$ and $\text{Pt/g-C}_3\text{N}_4$.